

Fractal Structure in Two-Dimensional Quantum Regge Calculus

Jun NISHIMURA* AND Masaki OSHIKAWA†

* *National Laboratory for High Energy Physics (KEK),
Tsukuba, Ibaraki 305, Japan*

† *Department of Applied Physics, University of Tokyo,
Bunkyo-ku, Tokyo 113, Japan*

Abstract

We study the fractal structure of the surface in two-dimensional quantum Regge calculus by performing Monte Carlo simulation with up to 200,000 triangles. The result can be compared with the universal scaling function obtained analytically in the continuum limit of dynamical triangulation, which provides us with a definite criterion whether Regge calculus serves as a proper regularization of quantum gravity. When the scale-invariant measure is taken as the measure of the link-length integration, we observe the correct scaling behavior in the data for the type of loop attached to a baby universe. The data seem to converge to the universal scaling function as the number of triangles is increased. The data for the type of loop attached to the mother universe, on the other hand, shows no scaling behavior up to the present size.

*E-mail address : nisimura@theory.kek.jp, JSPS Research Fellow.

†E-mail address : oshikawa@mmm.t.u-tokyo.ac.jp

Construction of a consistent theory of quantum gravity has been a long-standing problem in theoretical physics. Although we have not reached any satisfactory conclusion yet for the physically interesting four space-time dimensions, there has been considerable progress in two-dimensional quantum gravity [1], which is important not only as a toy model of four-dimensional quantum gravity, but also as a prototype of theories of strings or random surfaces. The progress is based on a continuum formulation — Liouville theory [2] — and a kind of lattice formulation — dynamical triangulation [3]. Both have been exactly solved and their equivalence has been shown up to the level of correlation functions [4].

In the case of ordinary quantum field theories, continuum formulations and lattice formulations have played complementary roles in understanding the universality in field theory. The details of lattice formulations at the lattice level are irrelevant to the long-range behavior of the theory, which can be also described in terms of a continuum formulation. A natural explanation of the universality has been given by the concepts of the renormalization group. The equivalence of Liouville theory and dynamical triangulation in two-dimensional quantum gravity suggests that the universality exists also in quantum gravity. In fact, some kinds of universality are known in dynamical triangulation; the continuum limit is not affected by using squares instead of triangles as the building blocks or by prohibiting tadpoles or self-energies in the dual diagram, etc.. Although we still lack understanding of the universality in quantum gravity in terms of the renormalization group, invention of such a framework (for some attempts, see [5]) might be especially useful in studying quantum gravity in three or four dimensions, where there is no analytic solution.

To this end, it seems quite important for us to investigate the universality phenomena further in two-dimensional quantum gravity. For example, there is a kind of lattice formulation of quantum gravity based on Regge calculus [6]. In this formulation, the lattice structure is fixed and the integration over the metric is replaced by the integration over the link lengths. An interesting question to ask here is whether two-dimensional Regge calculus falls into the same universality class as dynamical triangulation and Liouville theory. This is quite non-trivial, since it is questionable whether the general covariance arises in the continuum limit of such a system that can be viewed as a statistical model on a regular lattice. The answer is also desired from a practical point of view, since Regge calculus might be useful for numerical simulations of quantum gravity in higher dimensions.

Since analytic treatment of Regge calculus seems difficult beyond a perturbative expansion around flat space-time [7], we investigate the above issue by numerical simulation. There have been several works in this direction. A few years ago, Gross and Hamber [8] reported that Regge calculus reproduced the string susceptibility known in dynamical triangulation and in the continuum theory. Recently, Bock and Vink [9] have performed a more careful analysis and have claimed that Regge calculus fails to reproduce the desired string susceptibility. It has been also reported [8, 10] that the critical exponents of the Ising model on the dynamical Regge lattice agree quite well with the ones of the Ising model on the static lattice (Onsager's values) and not with the ones of the Ising model on the dynamically triangulated lattice. We think, however, that all these works are subject to some subtleties in Regge calculus concerning either the definition of string susceptibility or the introduction of matter fields, as we explain later.

In order to compare Regge calculus with the other approaches unambiguously, it is desirable to have a universal quantity which can be calculated directly from the geometry of

the surface. Indeed, such a quantity exists; it is the so-called loop-length distribution, which has been studied by Kawai, Kawamoto, Mogami and Watabiki [11]. They constructed a transfer-matrix formalism in dynamical triangulation. Using the formalism, they succeeded in obtaining the loop-length distribution in the continuum limit, which characterizes the fractal structure of the surface. The loop-length distribution can be defined unambiguously also in Regge calculus and it can be measured through numerical simulation. We, therefore, examine the loop-length distribution in a numerical simulation of Regge calculus and compare the result with that obtained in the continuum limit of dynamical triangulation.

Let us first explain the system we consider in this letter. In Regge calculus the dynamical variables are the link lengths on a fixed triangulation. Since it is essential for our purpose to have a spherical topology, we construct the fixed triangulation by dividing each of the twenty surfaces of an icosahedron into a triangular lattice. A tetrahedron or octahedron could be used as well, but we have chosen an icosahedron so that the artifact of the non-uniformity of coordination number may be the minimum. The integration over the link lengths is performed taking either the uniform measure $\int \prod_i dl_i$ or the scale-invariant measure $\int \prod_i dl_i/l_i$. The triangle inequality is imposed on every triangle. The total area is fixed to be equal to the number of triangles, so that the average area of a triangle in each configuration becomes unity. This can be realized in the simulation as follows. We first consider a system with the measure $\int \prod_i dl_i l_i^{p-1}$ and the action $S = \lambda A$, where A is the total area of the surface and λ is a constant parameter. $p = 1$ corresponds to the uniform measure and $p = 0$ corresponds to the scale-invariant measure. The partition function is given by

$$Z(\lambda) = \int \prod_i dl_i l_i^{p-1} e^{-\lambda A} \Theta(\text{triangle inequalities}), \quad (1)$$

where $\Theta(\text{triangle inequalities})$ is the step function which gives one if all the triangle inequalities are satisfied and zero otherwise. Changing the variables of integration as $l_i \rightarrow l_i/\sqrt{\lambda}$, one can extract the explicit λ -dependence of $Z(\lambda)$ as

$$Z(\lambda) = \frac{1}{(\sqrt{\lambda})^{pN_{\text{link}}}} \int \prod_i dl_i l_i^{p-1} e^{-A} \Theta(\text{triangle inequalities}), \quad (2)$$

where N_{link} is the number of links. Inverse Laplace transform of eq. (1) gives the distribution of the total area as

$$\varphi(A) \propto e^{-\lambda A} A^{\frac{pN_{\text{link}}}{2}-1}. \quad (3)$$

For the uniform measure ($p = 1$), we control the total area by introducing a positive λ , while for the scale-invariant measure ($p = 0$), we set $\lambda = 0$ and rescale the configuration whenever necessary during the simulation so that the total area may be kept within a range of moderate value. The configurations thus generated for either measure are each rescaled before measurements to have the fixed total area equal to the number of triangles. We have performed Monte Carlo simulations using the heat-bath algorithm with 50,000 triangles for the uniform measure and with 12,500, 50,000 and 200,000 triangles for the scale-invariant measure. The updating process in the program is vectorized since we can update one third of the links independently at the same time.

Before proceeding, we would like to explain the subtleties in Regge calculus. The first point is the definition of string susceptibility. In dynamical triangulation, the string susceptibility γ_{str} can be defined through

$$Z(N) = \sum_{T \in \mathcal{T}_N} e^{-S(T)} \sim N^{\gamma_{\text{str}}-3} e^{\kappa N} \quad (N \rightarrow \infty), \quad (4)$$

where \mathcal{T}_N denotes the set of triangulations with N triangles [12]. In Regge calculus, the partition function for a fixed triangulation with N triangles can be written as

$$Z(A, N) = \int d\mu(\{l_i\}) e^{-S(\{l_i\})} \delta(A(\{l_i\}) - A) \Theta(\text{triangle inequalities}), \quad (5)$$

where $d\mu(\{l_i\})$ denotes the measure for the link-length integration, and $A(\{l_i\})$ denotes the total area of the surface, which is fixed to a given value A . In refs. [8, 9], they defined the string susceptibility in Regge calculus through

$$Z(A, N) \sim A^{\gamma_{\text{str}}-3} e^{\kappa A} \quad (A \rightarrow \infty), \quad (6)$$

for a fixed N , which is taken to be sufficiently large. This definition of string susceptibility, however, might be too naive. When we consider a scaling relation in field theory, we have to keep the cutoff of the theory constant. In Regge calculus, we have no definite quantity that corresponds to the cutoff in ordinary field theory, and therefore the scaling argument is rather subtle. One natural thing to do is to consider the average area of a triangle in each configuration as the cutoff in ordinary field theory. In order to keep the cutoff constant, say at unity, we should fix the total area A to be equal to the number of triangles N . The string susceptibility, then, can be defined through

$$Z(A = N, N) \sim N^{\gamma_{\text{str}}-3} e^{\kappa N} \quad (N \rightarrow \infty). \quad (7)$$

Unfortunately, the string susceptibility thus defined seems to be difficult to extract from numerical simulation, since we have to probe the difference in free energy for different numbers of triangles. The second point is the introduction of matter fields. If we assign a single spin to each triangle, each spin should be regarded as a representative (“block spin”) of the dynamical degrees of freedom within the triangle. Therefore, we may have to, for example, make the Ising coupling constant dependent on the size of the triangle, which takes a different value from point to point in Regge calculus. Thus the negative results obtained in ref. [8, 10] might be due to the problem of the action for the matter fields. In contrast to the above points, the loop-length distribution can be defined unambiguously in Regge calculus and we hope this provides us with a definite criterion whether Regge calculus serves as a proper regularization of quantum gravity.

Let us explain the loop-length distribution, which plays a central role in our study. The set of points which are at a distance D from a given point is composed of a number of disconnected closed loops. The distribution $\rho(L, D)$ of the loop length L at the distance D has been obtained in the continuum limit of dynamical triangulation as [11]

$$\rho(L, D) = \frac{1}{D^2} f(x) \quad (8)$$

$$f(x) = \frac{3}{7\sqrt{\pi}} \left(x^{-\frac{5}{2}} + \frac{1}{2} x^{-\frac{3}{2}} + \frac{14}{3} x^{\frac{1}{2}} \right) e^{-x}, \quad (9)$$

where $x = L/D^2$. The fact that such a quantity does possess a sensible continuum limit is not only quite non-trivial itself but also of great significance since it provides us with a geometrical picture of the continuum limit of quantum gravity. It implies that in the continuum limit of quantum gravity, the space-time becomes fractal in the sense that sections of the surface at different distances from a given point look exactly the same after a proper rescaling of loop lengths. Let us here consider the distribution of loops with length L attached to a universe with area A' . This can be written in terms of the functions given in ref. [11] as,

$$\rho(L, A'; D; A) = \lim_{L_0 \rightarrow 0} \frac{\frac{1}{2\pi i} \int d\tau' N(L_0, L; D; \tau') e^{\tau'(A-A')} \frac{1}{2\pi i} \int d\tau'' \frac{1}{L} F(L, \tau'') e^{\tau'' A'}}{\frac{1}{2\pi i} \int d\tau'' \frac{1}{L_0} F(L_0, \tau'') e^{\tau'' A}}, \quad (10)$$

where A is the total area of the surface. When we take the thermodynamic limit $A \rightarrow \infty$, we can fix either A' or $(A - A')$ to a finite value B . The former corresponds to the type of loop attached to a baby universe, while the latter corresponds to the type of loop attached to the mother universe. We refer to the two types of loops simply as “baby” loops and “mother” loops, respectively (fig. 1). Note that baby loops are not necessarily smaller than mother loops. The distribution for baby loops can be calculated as follows,

$$\rho_b(L, B; D) = \frac{1}{2\pi i} \int d\tau' e^{\tau' B} \lim_{L_0 \rightarrow 0, \tau \rightarrow 0} \frac{\frac{\partial^2}{\partial \tau^2} N(L_0, L; D; \tau) \frac{1}{L} F(L, \tau + \tau')}{\frac{\partial^2}{\partial \tau^2} \frac{1}{L_0} F(L_0, \tau)} \quad (11)$$

$$= \frac{1}{D^6} \frac{6}{7\pi} \left(1 + \frac{1}{2}x\right) e^{-x} x^{\frac{1}{2}} y^{-5} e^{-\left(\frac{x}{y}\right)^2}, \quad (12)$$

where $x = L/D^2$ and $y = \sqrt{B}/D^2$. Integrating over B , one gets,

$$\rho_b(L, D) = \int_0^\infty \rho_b(L, B; D) dB \quad (13)$$

$$= \frac{1}{D^2} f_b(x), \quad (14)$$

where

$$f_b(x) = \frac{3}{7\sqrt{\pi}} \left(x^{-\frac{5}{2}} + \frac{1}{2}x^{-\frac{3}{2}}\right) e^{-x}. \quad (15)$$

The distribution for mother loops can be calculated similarly.

$$\rho_m(L, B; D) = \frac{1}{2\pi i} \int d\tau' e^{\tau' B} \lim_{L_0 \rightarrow 0, \tau \rightarrow 0} \frac{\frac{\partial^2}{\partial \tau^2} N(L_0, L; D; \tau + \tau') \frac{1}{L} F(L, \tau)}{\frac{\partial^2}{\partial \tau^2} \frac{1}{L_0} F(L_0, \tau)} \quad (16)$$

$$= \frac{1}{\sqrt{\pi L}} \frac{\partial}{\partial D} \left[\frac{1}{2\pi i} \int_{-i\infty}^{i\infty} d\tau e^{\tau B} \exp \left\{ -\frac{\sqrt{\tau} L}{2} \left(3 \tanh^{-2} \frac{\sqrt{6\sqrt{\tau} D}}{2} - 2 \right) \right\} \right] \quad (17)$$

Integrating over B , one gets,

$$\rho_m(L, D) = \int_0^\infty \rho_m(L, B; D) dB \quad (18)$$

$$= \frac{1}{\sqrt{\pi L}} \frac{\partial}{\partial D} \lim_{\tau \rightarrow 0} \exp \left\{ -\frac{\sqrt{\tau} L}{2} \left(3 \tanh^{-2} \frac{\sqrt{6\sqrt{\tau} D}}{2} - 2 \right) \right\} \quad (19)$$

$$= \frac{1}{D^2} f_m(x), \quad (20)$$

where

$$f_m(x) = \frac{2}{\sqrt{\pi}} x^{\frac{1}{2}} e^{-x}. \quad (21)$$

The total distribution reproduces the result of ref. [11]¹, *i.e.* $\rho(L, D) = \rho_b(L, D) + \rho_m(L, D)$. Note that the integration of the mother-loop distribution over L gives

$$\int_0^\infty \rho_m(L, D) dL = \frac{2}{\sqrt{\pi}} \int_0^\infty x^{\frac{1}{2}} e^{-x} dx = 1, \quad (22)$$

which means that one finds exactly one mother loop at a fixed D in each configuration.

In Regge calculus we define the loop-length distribution in the following way. Representing each triangle by the center of its inscribed circle, we define the length of a dual-link by the geodesic distance of the two representative points at the ends of the dual-link. Then we define the distance between two given triangles by the length of the shortest dual-link path connecting the two triangles (fig. 2). The boundary between triangles at a distance less than or equal to D from a given triangle and those at a distance greater than D from the same triangle is composed of disconnected closed loops, whose lengths are defined by summing up the lengths of the links forming each loop. This gives the definition of the loop-length distribution in Regge calculus. Since we are dealing with a finite number of triangles, we have a maximum D at which all the triangles are included. We measure the loop-length distribution at D 's which are less than half of the maximum D . Also the finiteness of the system makes the classification of loops into baby loops and mother loops somewhat ambiguous. We identify the mother loop with the loop attached to the largest universe at a fixed D . The measurement has been made every 200 sweeps, and at each measurement we choose ten triangles randomly as the starting point of the distance D in order to increase the statistics. The number of sweeps required for the thermalization of the data is large for the scale-invariant measure; *e.g.* 500,000 sweeps in the case of 12,500 triangles.

Let us show the results of our simulation. The data for the uniform measure ($\int \prod_i dl_i$) with 50,000 triangles is shown in Fig. 3. The loop-length distribution is plotted against the scaling variable $x = L/D^2$ for $D = 20, 40, 60, 80, 100, 120$, where L is the length of the loop and D is the distance from a point on the surface. The result does not show any scaling behavior in terms of x for different values of D . The distribution for each D is split into two parts: the left one which corresponds to baby loops and the right one which corresponds to mother loops. One should note that it is a log-log plot, and so we see that the baby loops are extremely suppressed. Indeed, for most cases we find only one loop, which is the mother loop, for each D in a configuration. (A baby loop appears on average only once in five configurations even for $D = 120$.) This means that the surface is rather similar to a smooth sphere, where always only one loop (which is the mother loop) appears. Hence the surface is quite different from being fractal as in dynamical triangulation, where many loops appear for each D .

¹The fact that the loop-length distribution is composed of two such contributions can also be seen from eq.(24) of ref. [11]. One can get the singularity $\tau^{3/2}$ in the numerator either from the proper-time evolution kernel $N(L_0, L; D)$ or from the disk amplitude $F(L)$. The former contribution corresponds to baby loops, while the latter to mother loops [13].

The data for the scale-invariant measure ($\int \prod_i dl_i/l_i$) with 12,500 triangles is shown in Fig. 4. The loop-length distribution is plotted against the scaling variable $x = L/D^2$ for $D = 10, 15, 20$. Something of a scaling behavior is seen in the intermediate region of x . To clarify the situation, we separate the two contributions, the one from baby loops and the one from mother loops. The distribution for baby loops is shown in Fig. 5. A clear scaling behavior can be seen with $x = L/D^2$ as a scaling parameter. Furthermore, we compare our result with the universal function (15) obtained in the continuum limit of dynamical triangulation. Since there is an ambiguity by a constant factor between the scaling parameter x in our system and that in eq. (15), we fit our result with $\alpha f_b(\alpha x)$, where α is the fitting parameter. The best fit ($\alpha = 3.2$) is shown by the dotted line in Fig. 5. Our data is in good agreement with the universal function. Let us see how the slight discrepancy seen in the small- x region behaves as we increase the number of triangles N . Fig. 6 shows the results for $D = 20$ with 12,500, 50,000 and 200,000 triangles. We find that the data curve in the small- x region approaches to the curve of the universal function (15). Thus we expect that the distribution of baby loops will converge to the universal function in the $N \rightarrow \infty$ limit. The distribution for mother loops, on the other hand, is shown in Fig. 7 and Fig. 8, which correspond to the cases with 12,500 triangles and 200,000 triangles respectively. We cannot see any scaling behavior here. The dotted line represents the rescaled universal function $\alpha f_m(\alpha x)$ with the same $\alpha = 3.2$ that gives the best fit in the case of the baby-loop distribution. Although we might expect that the data will approach the universal function for larger D with sufficiently many triangles, the finite-size effect in the present data is too severe for us to draw any conclusion.

To summarize, we have performed a Monte Carlo simulation of two-dimensional Regge calculus up to 200,000 triangles and measured the loop-length distribution, which is the distribution function of the length L of the loops whose geodesic distance from a point is a constant D . The results are compared with that obtained in the continuum limit of dynamical triangulation, which has the scaling behavior in terms of $x = L/D^2$.

For the uniform measure ($\int \prod_i dl_i$), we find no scaling in terms of x at the present size. Moreover, we find for most cases only one loop for each D . This means that the surface is smooth, in contrast to the fractal structure in dynamical triangulation.

For the scale-invariant measure ($\int \prod_i dl_i/l_i$), we find that the baby-loop distribution shows a clear scaling behavior in terms of x , which is in good agreement with the universal function obtained in the continuum limit of dynamical triangulation. It is rather surprising that Regge calculus and dynamical triangulation, which seem to be quite different systems, show the same universal behavior at least for the baby-loop distribution. It is not clear at present whether the scale-invariant measure is essential in obtaining this universal behavior. One might expect that if there is a universality at all, the choice of the measure of the link-length integration would be irrelevant to the universal behavior. We should note, however, that the scale-invariant measure is very special, as is seen in eq. (3). It implies that the fluctuation of the area of each triangle becomes overwhelmingly large when the scale-invariant measure is adopted. Since the lattice structure is regular in Regge calculus, such a large fluctuation might be necessary to obtain a fractal structure as in dynamical triangulation.

As for the mother-loop distribution, the situation is not clear even for the scale-invariant

measure. We feel it is possible that the mother-loop distribution, as well as the baby-loop distribution, converges to the universal function in the $N \rightarrow \infty$ limit. Even if this turns out to be the case, we may at least say that Regge calculus requires many more triangles in order to obtain the universal behavior than dynamical triangulation, which is known to show a fairly good universal fractal structure with no more than 20,000 triangles [14].

We would like to thank H. Kawai for stimulating discussions and for continuous encouragement. It is our pleasure to acknowledge M. Ninomiya, M. Fukuma and M. Oogami for useful comments. We are also grateful to T. Yukawa and N. Tsuda for providing us with their unpublished data of loop-length distribution in two-dimensional dynamical triangulation and to N. McDougall for carefully reading the manuscript. The calculations were carried out on the supercomputer HITAC S820/80 at National Laboratory for High Energy Physics(KEK).

References

- [1] A.M. Polyakov, Mod. Phys. Lett. **A2** (1987) 893.
V.G. Knizhnik, A.M. Polyakov and A.B. Zamolodchikov, Mod. Phys. Lett. **A3** (1988) 819.
- [2] F. David, Mod. Phys. Lett. **A3** (1988) 1651.
J. Distler and H. Kawai, Nucl. Phys. **B321** (1989) 504.
- [3] E. Brézin, C. Itzykson, G. Parisi and J.-B. Zuber, Commun. Math. Phys. **59** (1978) 35.
F. David, Nucl. Phys. **B257** (1985) 45.
V.A. Kazakov, Phys. Lett. **150B** (1985) 282.
D.V. Boulatov, V.A. Kazakov, I.K. Kostov and A.A. Migdal, Nucl. Phys. **B275** (1986) 641.
J. Ambjørn, B. Durhuus and J. Fröhlich, Nucl. Phys. **B257** (1985) 433.
- [4] M. Goulian and M. Li, Phys. Rev. Lett. **66** (1991) 2051.
Y. Kitazawa, Phys. Lett. **B265** (1991) 262.
P. Di Francesco and D. Kutasov, Phys. Lett. **B261** (1991) 385.
Vl. S. Dotsenko, Mod. Phys. Lett. **A6** (1991) 3601.
K.-J. Hamada, preprint YITP/U-93-28, to appear in Nucl. Phys. **B**, preprint YITP/U-93-34.
- [5] J. Nishimura, N. Tsuda and T. Yukawa, Prog. Theor. Phys. (Suppl.) **114** (1993) 19.
R.L. Renken, hep-lat/9405007, April 1994.
- [6] T. Regge, Nuovo Cimento **19** (1961) 558.
- [7] H.W. Hamber, Les Houches, Session XLIII (1984), K. Osterwalder and R. Stora, eds. and references therein.
- [8] M. Gross and H.W. Hamber, Nucl. Phys. **B364** (1991) 703.
- [9] W. Bock and J.C. Vink, UCSD/PTH 94-08, hep-lat/9406018, June 1994.
- [10] C. Holm and W. Janke, FUB-HEP 06/94, hep-lat/9406020, June 1994.
- [11] H. Kawai, N. Kawamoto, T. Mogami and Y. Watabiki, Phys. Lett. **B306** (1993) 19.
- [12] For numerical extraction of the string susceptibility in dynamical triangulation, see :
J. Ambjørn, S. Jain and G. Thorleifsson, Phys. Lett. **B307** (1993) 34.
- [13] H. Kawai, private communication.
- [14] N. Tsuda and T. Yukawa, Phys. Lett. **B305** (1993) 223.

Figure captions

Fig. 1 The loops appearing at the distance D from a given point. There are two types of loops : the “mother” loop which is attached to the mother universe, and “baby” loops which are attached to baby universes.

Fig. 2 An example of a dual-link path connecting the two shaded triangles. The distance between the two triangles is defined by the length of the shortest dual-link path.

Fig. 3 The loop-length distribution for the uniform measure ($\int \prod_i dl_i$) with 50,000 triangles. The horizontal axis is the scaling variable $x = L/D^2$.

Fig. 4 The loop-length distribution for the scale-invariant measure ($\int \prod_i dl_i/l_i$) with 12,500 triangles. The horizontal axis is the scaling variable $x = L/D^2$. The dotted curve is the rescaled universal function $\alpha f(\alpha x)$ with the same $\alpha = 3.2$ that gives the best fit in the case of the baby-loop distribution (Fig. 5).

Fig. 5 The baby-loop length distribution for the scale-invariant measure ($\int \prod_i dl_i/l_i$) at $D = 10, 15, 20$ with 12,500 triangles. The horizontal axis is the scaling variable $x = L/D^2$. The dotted curve is the rescaled universal function $\alpha f_b(\alpha x)$ with $\alpha = 3.2$ which gives the best fit.

Fig. 6 The baby-loop length distribution for the scale-invariant measure ($\int \prod_i dl_i/l_i$) at $D = 20$ with 12,500, 50,000, 200,000 triangles. The horizontal axis is the scaling variable $x = L/D^2$.

Fig. 7 The mother-loop length distribution for the scale-invariant measure ($\int \prod_i dl_i/l_i$) at $D = 10, 15, 20$ with 12,500 triangles. The horizontal axis is the scaling variable $x = L/D^2$. The dotted curve is the rescaled universal function $\alpha f_m(\alpha x)$ with the same $\alpha = 3.2$ that gives the best fit in the case of the baby-loop distribution.

Fig. 8 The mother-loop length distribution for the scale-invariant measure ($\int \prod_i dl_i/l_i$) at $D = 20, 40, 60$ with 200,000 triangles. The horizontal axis is the scaling variable $x = L/D^2$.

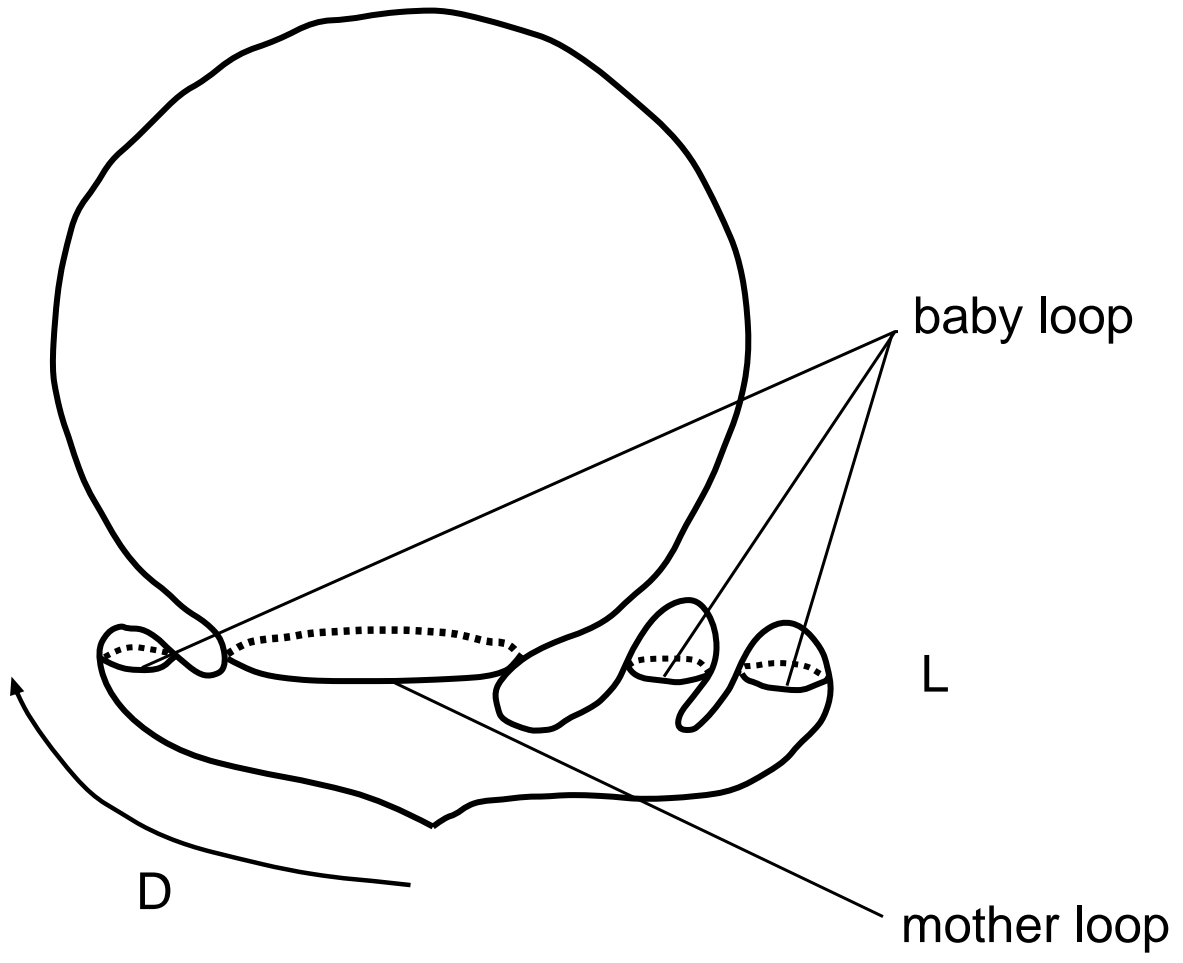


fig. 1

This figure "fig1-1.png" is available in "png" format from:

<http://arxiv.org/ps/hep-lat/9407016v2>

This figure "fig2-1.png" is available in "png" format from:

<http://arxiv.org/ps/hep-lat/9407016v2>

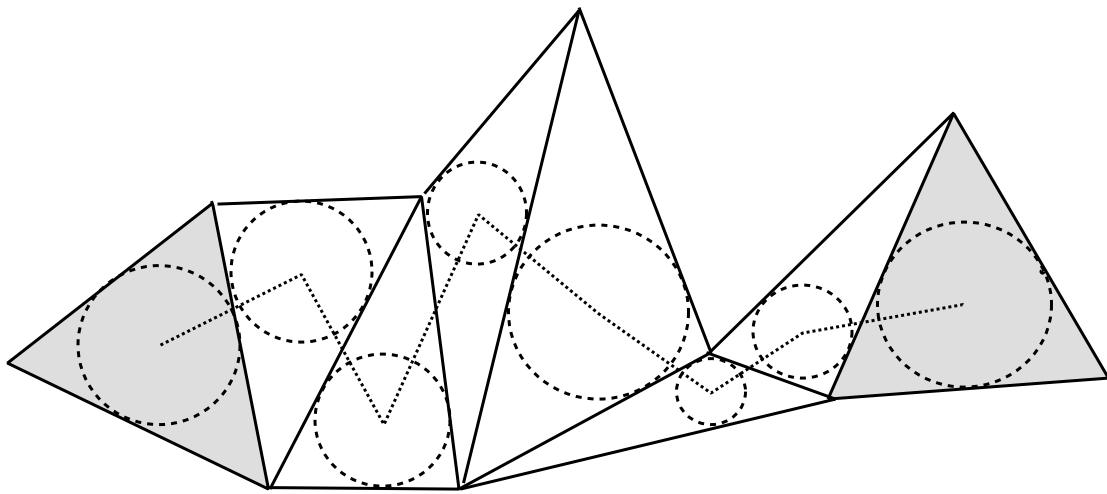


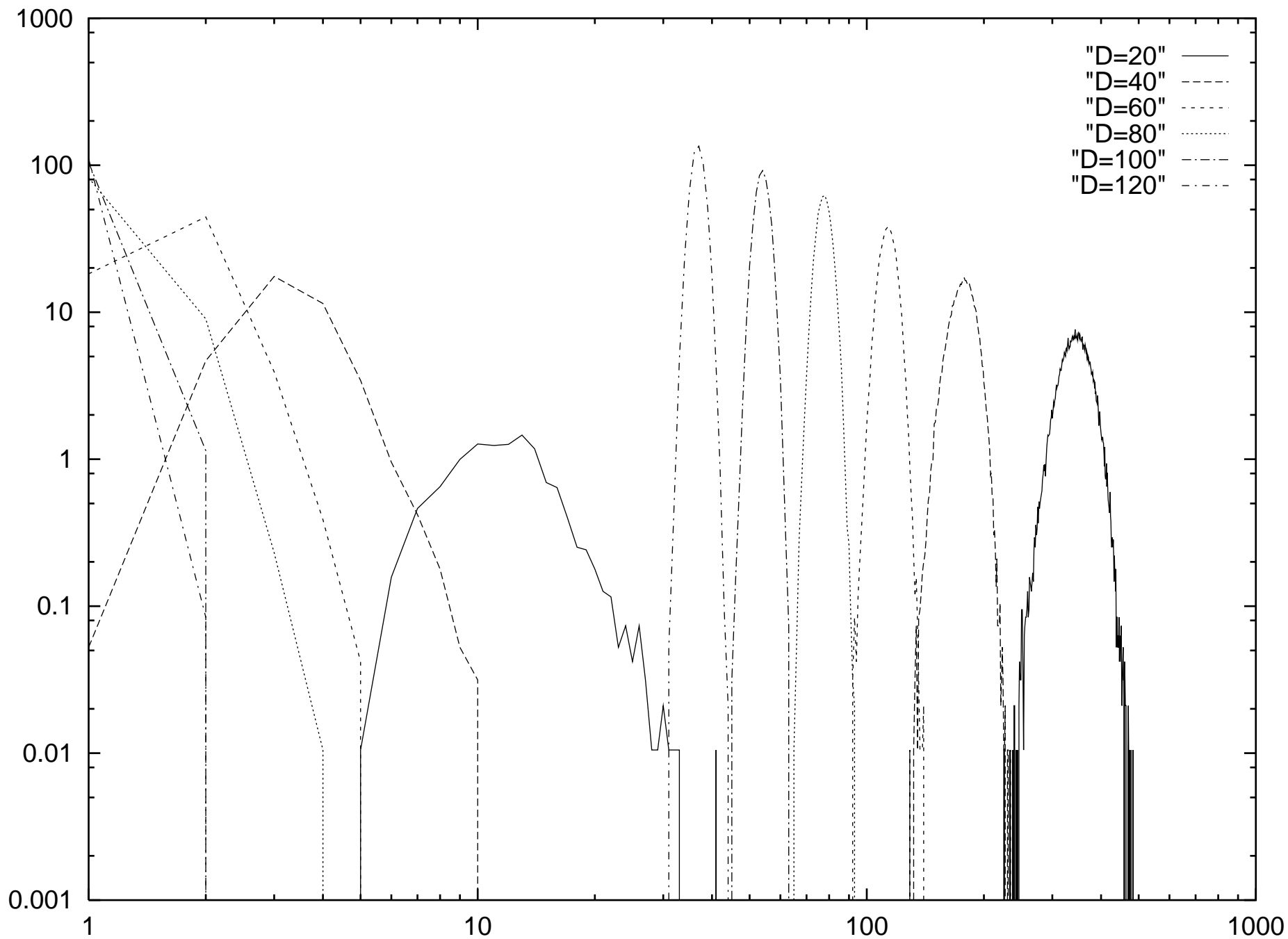
fig. 2

This figure "fig1-2.png" is available in "png" format from:

<http://arxiv.org/ps/hep-lat/9407016v2>

This figure "fig2-2.png" is available in "png" format from:

<http://arxiv.org/ps/hep-lat/9407016v2>

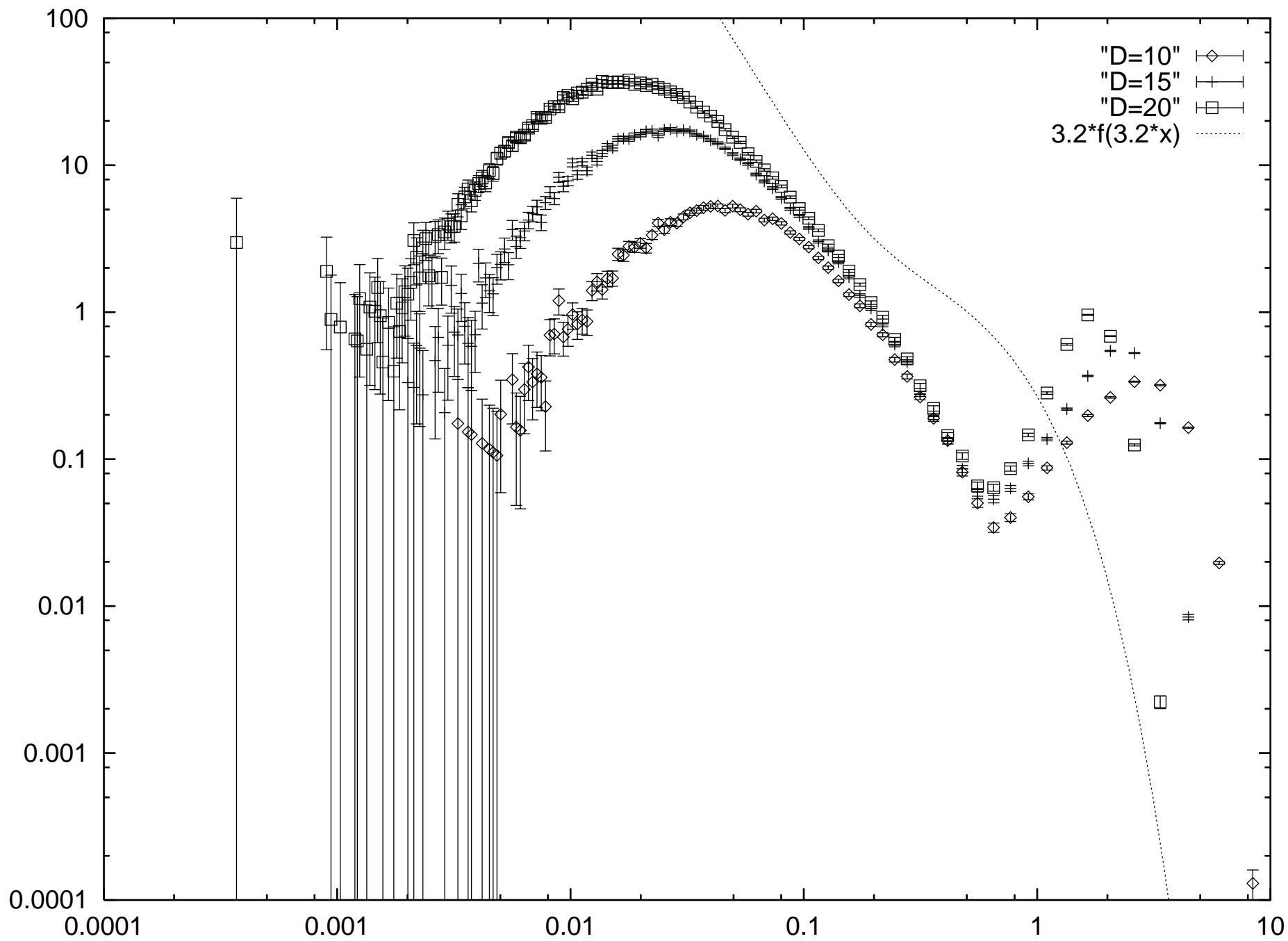


This figure "fig1-3.png" is available in "png" format from:

<http://arxiv.org/ps/hep-lat/9407016v2>

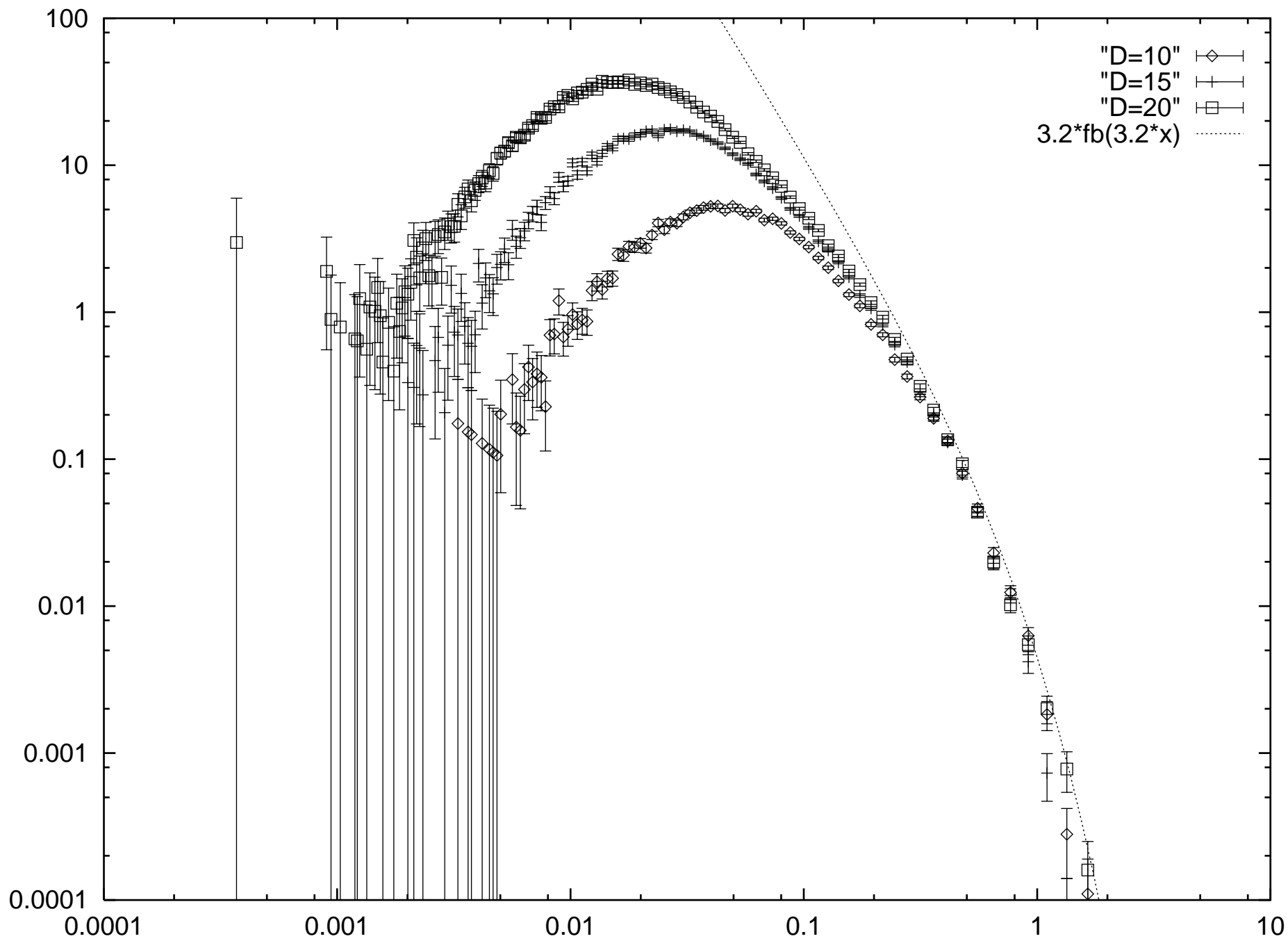
This figure "fig2-3.png" is available in "png" format from:

<http://arxiv.org/ps/hep-lat/9407016v2>



This figure "fig1-4.png" is available in "png" format from:

<http://arxiv.org/ps/hep-lat/9407016v2>



This figure "fig1-5.png" is available in "png" format from:

<http://arxiv.org/ps/hep-lat/9407016v2>

